
# POLITECNICO DI TORINO

*Department of Environment, Land and Infrastructure Engineering*

Master of Science in Petroleum Engineering

## Coupled Hydro-Mechanical Simulations For Heterogeneous Fractured Reservoirs

Supervisors:

Prof. Chiara Deangeli

Nicolas Ishac

Prof. Hamid Nick

Prof. Saeed Salimzadeh

**December 2018**

Thesis submitted in compliance with the requirements for the Master of Science degree

# Acknowledgements

I would like to thank my supervisor, Professor Chiara Deangeli for the support and collaboration during this process, always being able to help and ensuring a successful completion of the work

Special thanks to the Danish Hydrocarbon Research And Technology Centre of the Technical University Of Denmark (DTU) , primarily to my supervisors Hamid Nick and Saeed Salimzadeh, whom always are ready to collaborate showing passion and dedication in their work. Thank you for all the explanations and time invested in the students.

I would also like to thank my fellow students and friends for motivation, encouragement and good fun during my time as a student. Finally, I must express my gratitude to my family for always supporting me. Thank you.

# Abstract:

Predicting equivalent permeability in fractured reservoirs requires an analysis of the fractures network geometry and apertures. A good understanding of the fracture network implies understanding of fracture location, orientation, and connectivity which is the key point to fractured reservoir characterization. Transport properties in the fractures strongly depend on the aperture size and its distribution, thus the ability to investigate fracture aperture would provide extensive amount of information for reservoir characterization and monitoring. This work investigates, using numerical modelling, the effect of aperture heterogeneity on the flow through a fractured network. A fully coupled hydro-mechanical (HM) finite element model is used to reconstruct the behavior of the fracture aperture. The model accounts for the mechanical deformation, related to the change in the external stress which cause alteration of the fracture aperture. It accounts also for the fluid flow in the fractures and rock matrix. Fracture were generated according to a computational model developed by a previous research (Welch et al., 2018). This study shows that aperture heterogeneity tends to overestimate the equivalent permeability of a fracture network. In order to describe the heterogeneity behavior, a permeability ratio, K Homogeneous/ K heterogeneous, was introduced that represents the equivalent permeability of the network assuming uniform aperture over the equivalent permeability of the same network assuming heterogeneous aperture. Results showed that this ratio increases with increasing fracture density, up to a threshold where it starts to decreases again, where accounting for aperture heterogeneity became negligible at high density network. The reason for this behavior is because the fluid tends to select a path through the most transmissive fracture; as more fracture intersect themselves, they offer additional larger transmissivity shortcuts and deviations, enhancing thus the equivalent network permeability and neglecting the effect of heterogeneity.

# Contents

# List of Figures

# List of Tables

# Chapter 1: Introduction

## 1.1 Overview

Modelling naturally fractured reservoirs requires mapping fracture network and estimation of their properties such as porosity and permeability (Berkowitz et al., 2002). These tasks are not easy to achieve, as the data are mostly limited to well scale measurement, outcrops studies and seismic maps. In other words, more information are required. Thus, for a static modelling, any data extracted from these sources about fracture network studies are crucial to initiate the modelling preparation in order to be able to achieve accurate assessment of reservoir performance. Permeability is considered the most challenging parameter to be analyses. Despite the vast work on characterizing fractured rocks studied over the last few decades, predicting fluid flow within the host rocks is still a challenging work (Ebigbo et al., 2016 ).

Naturally fractured reservoir are regarded as heterogeneous porous media often found in sandstones, carbonate reservoirs and other formations (Jaafari et al., 2013). The matrix system which are mostly the main part of a fractured reservoir have low permeability and high storage volume while the fracture system have high permeability but contains very little fluid. Therefore, the rock matrix acts as the primary source of hydrocarbon and the fracture serves as the main path for fluid flow. Reservoir are recognized as primary ``fractured ´´ if the fractures form an interconnected network (Bogdanov et al., 2007). Fractures that are more permeable than host rock can act as preferential or at least additional pathways for fluid to flow through the rock which is relevant in several areas of earth science and engineering, exploitation of hydrocarbons, geothermal reservoirs, and hydraulic fracturing (Saeed et al., 2017). Recently, it attracted the attention in connection with the problem of geological isolation of radioactive waste (Ji et al., 2011). Natural fracture media displays a strong hydraulic complexity coming from the arrangement of the fractures in complex networks, their interaction with the environing rock matrix (Dreuzy et al., 2012). Thus, the contribution of flow through fracture to total reservoir flow is difficult to analyses, and in predicting the flow through fractured rock, the effective permeability is a crucial parameter as it requires understanding the 3-D fracture

geometry network and depends on many properties (Jarrahi et al., 2017). The range influence of fracture can be attributed to their spatial variations in fracture density, orientation, aperture, spacing and conductivity (Li et al., 2018). Fracture network connectivity and fracture aperture distribution are the two key factor which dominate flow behavior in fracture network. In fact, Fracture connectivity could be used to study most of the fundamental properties of fracture network (Sun et al., 2014). It can be evaluated by the percolation theory which is a powerful tool for analyzing numerous transport phenomenon of rocks (Ma et al., 2017).

Fracture aperture is less commonly investigated, and the spatial heterogeneity, ubiquitous in geologic formations, strongly affects the flow behavior as small variation in aperture have large implication on rock flow and transport properties which might lead to large incertitude in fluid flow modeling (Guo et al., 2016). Estimation of aperture is provided through borehole imaging tool but with uncertainty because of the absence of accurate calibration (Bisdom et al., 2016). Most of the previous fractures model assumed parallel plate fracture or smooth fracture and fracture properties such as permeability were easily estimated. However, those model were idealized and further improvement were required in order to match the available geological and well logging data. One has to investigate whether large aperture, long fracture dominate performance of compared to short, small aperture. The aperture of a rock fracture can be statistically represented by a spatially auto correlated random field as The apertures of a fracture had been found to typically follow under a given state of stress the gamma distribution or the log-normal distribution or a truncated Gaussian distribution (Guo et al., 2016). The ability to understand and predict the reservoir response became essential part of a good sustainable exploitation. Recently, with the increase and the advance in measuring computer power and equipment, the oil and gas as well as the geothermal industries are presented with some of today most complex data science problem (Roland et al., 2018). Thus, statistical methods are becoming crucial tools for a diagnosing analysis in the exploration, production and delivery phases. There have been improvement over the years in: representation of fluids in the reservoir, modelling of fluid flow between fractures and matrix blocks, modelling of fluid flow between matrix blocks in adjacent computational grid blocks, and discretization of the matrix block (Roland et al., 2018). Different approaches were proposed to characterize naturally fractured reservoirs. The discrete fracture network (DFN) model fracture for flow analysis because of its simplicity to implement and it allows for an improved integration of the geological

data into the flow models (Dreuzy et al., 2012). DFN simulate fractured media by modeling each fracture individually. Therefore, Flow properties from large geological and geophysical data present on fracture media can be extracted. The DFN uses the assumption that the rock matrix is extremely low and can be neglected. Due to computing limitation, this assumption was acceptable and matrix permeability could be ignored but with the recent advance in earth science in the past few years, accuracy and reliability in predicting overall permeability became more important and matrix permeability cannot be neglected. In our model we will refer to it as discrete fracture and matrix (DFM) in which matrix blocks are modeled with permeable boundaries and the fracture system is modeled with DFN. Other models to represent matrix fracture include the dual continuum method, double and multi-porosity and the effective continuum model

## 1.2 Background on percolation theory

The percolation theory, used to describe the connectivity and conductivity, is a powerful mathematical tool to analyses various phenomena in disorder media, especially in controlling fluid transport in complex systems (Berkowitz et al., 2002). For example, Long and Billaux observed that, due to low fracture connectivity at afield site in France, more or less 0.1% of fractures contribute to the overall fluid flow. In other words, most of fractures can be removed without significantly affecting the effective permeability of the network. This parameter, however, is not easy to quantify. For this reason, one has to defined what is a good definition of a ``fractured'' network. Berkowitz et al. (2002) reported that even domains that appear to be extremely fractured may not be in fact well connected. In a fractured rock mass, some fractures are isolated while others intersect. This depends on the fracture density (low, medium, high). As the fracture density becomes higher, many connect until a large cluster form. When this cluster intersects all boundaries of the simulated area, a continuous percolation forms and the point at which the cluster connects is defined as the threshold density. Thus, a connected network is above the percolation threshold. Dreuzy et al. (2012) stated that below the percolation threshold, the hydraulic properties are neither determined by the network structure nor the fracture internal characteristiques but rather by the matrix properties. They believes dense networks are those with a fracture density above the percolation threshold and sparse as the one below. Contrary, Berkowitz supposes that dense network fracture might not hydraulically connected, as the

network can be near the percolation theory. This difference in opinion is due to data uncertainty. Masihi et al. (2010) studied the percolation threshold of fracture density with different length distributions and system sizes. He found out that the percolation threshold for a fracture network with two perpendicular fractures sets is lower than a fracture model with fractures that are randomly oriented. Berkowiz found consistency with their case. The power law relationship derived in percolation theory normally takes the form of A proportional to $(N-N_c)^{-x}$ where A is the geometrical or physical quantity ( such as hydraulic conductivity), x is the exponent specific to quantity A, N the total number of fracture and $N_c$ the critical number of fractures at threshold. Power law of this forms have found to characterize geometrical characteristic and flow properties of fracture networks, such as the density of the fracture to ensure network connectivity (Jaafari et al., 2013) . The percolation Threshold is not our focus in this paper as we wanted to investigate on less studied problem related to the aperture heterogeneity of the fracture network.

## 1.3 Matrix Permeability:

Matrix permeability is becoming important in fractured reservoir modelling. The effect of fracture decrease with increasing matrix permeability (Vik et al., 2018). Bisdom et al. (2016) presented a model to investigate the contribution of fracture flow on equivalent permeability as a function of aperture definitions and matrix permeability by comparing the impact of 3 different aperture models on the equivalent permeability. In their research, using the power law aperture frequency scaling , fracture increase permeability up to 60 % and their impact decrease when the matrix increase up to 1 Darcy, while using the linear length scaling method the impact of fracture on does not change due to the high contrast between fracture and matrix ( equivalent permeability 4 times the matrix one). Finally, using the Barton- Bandis distribution, the impact of fractures is low for a 1000 Darcy mD matrix permeability. These differences are due to the fraction of the critically stressed fracture which has strong effect on the intra-fracture connectivity. Matthai et al. (2004) similarly studied the influence of fracture on the matrix's one and found that when fracture over matrix's permeability KF/KM less than $10^2$ the impact of fracture is negligible. When the ratio exceed $10^3$-$10^4$, fractures strongly perturbate the flow and when once it reached $10^5$-$10^6$ fractures carries all the flow.

Namdari et al. (2016) compare DFN and DFM and found even for low aperture 17 % higher permeability was resulted when accounting for matrix permeability.

## 1.4. Aperture

The first approximation of modelling aperture was the parallel plate, and early modeling showed deviation from the model of identical mean aperture, as deviation increase fracture closure and results in heterogeneity which induce flow channeling (Guo et al., 2016) .Dreuzy et al. (2012) refers that the spatially correlated fluctuation of aperture permit the existence of either correlated large aperture channels and low aperture barriers which impact the permeability. Numerical simulation shows that aperture can ease the flow through the fracture and make it more permeable than the parallel plate assumption or hinder the flow and establish bottleneck. They considered both heterogeneity in fracture scale and network scale with static loading and isotropic stresses. In their paper, they introduce the critical closure ratio closure $\sigma/a_m$ and believe that it is the key parameter that controls the heterogeneity, with σ the standard deviation of the truncated distribution and am the mechanical aperture. At Fracture scale, heterogeneity aggravate the flow because of the higher possibility of generation obstacles and for the network scale it can either increase for long and dense networks or decrease for short and sparse 'one. The role of the correlation length, which represent a measure in length over which the fracture aperture value at one location is correlated with its neighboring points has been little researched. Guao et al. (2016) found that when the correlation length is 1/5 lower than the well distance, a heterogeneous fracture behave as a homogeneous one. They studied the effect of spatial heterogeneity in a single fracture on flow during heat production from EGS using the standard deviation and correlation length. Their results showed also that the effect of varying the standard deviation is negligible for short correlation length as heterogeneity will not have any impact. Also, the initial aperture field with greater standard deviation enables more distinct preferential paths, and it is more likely to develop a dominant flow channel rather than multiple preferential paths.

Gong et al. (2017) analyze how broad the aperture distribution should be that a well-connected fracture can exhibit a sparse critical sub network with the same permeability. He founds that the fracture network with aperture distribution that follows power law or log normal, if the network is well connected most of the fracture can be removed without affecting the equivalent permeability and when the standard deviation is decreases, fewer can be removed without reducing the equivalent permeability. Bisdom et al . (2016) analyze the impact of 3 different methods to predict kinematic aperture and 2 critical stress criteria and found that linear length aperture scaling predicts the largest kinematic aperture and the Barton Bandis predicts that 80

% of the fracture are critically stressed while coulomb 50 % as coulomb does not incorporate length and spacing into the critical stress analysis. Another study related to aperture shrinkage was done by Canbolat et al. (2018) showed decrease in fracture aperture after the injection of polymer gel conformance to improve the recovery. Zuang et al. (2013) had studied the effect of aperture distribution for two phase flow occurring in rough walled rock fractured and found that for fractures with high spatial correlation continuous flow paths can be easily form with smaller aperture for wetting phase or with larger aperture for non-wetting phase.

## 1.5. Coupled T-H-M

Experimental and theoretical studies has showed the last few years progress related to the effect of coupling Temperature, Hydrologic flow, and mechanical deformation (THM) in fractured rock. THM processes are important in several areas including geothermal energy extraction, gas production from coal beds, seismicity induced by fluid injection, and injection pressure needed for stimulation deep petroleum reservoir with water cold than in situ fluids (Cladouhous et al., 2010). Up to date the coupling of THM processes is a main challenge to the geoscience industry as those processes have different characteristic spatial and time scales. The mechanical response in a rock can propagate through the rock mass with the speed of elastic waves and the presence of fracture control the deformability. Thus, the mechanical effects have short time scale. Thermal effect on the other hand have long spatial and time scale. The volumetric flow rate for a fracture is proportional to the pressure gradient and the cube of the fracture aperture which is derived from the general navier stock equation for flow of a liquid in 2 parallel plates (Sarkar et al., 2004). Hence variation in fracture aperture due to changes in the normal or shear stresses acting on the fracture surface as a result of THM processes have a big impact on the fluid flow and heat transport in a fracture. Saeed et al. (2018) presented a couple THM model for deformable fractured geothermal reservoir and their results showed The fluid exchange heat with the rock. .matrix which lead to cooling down of the matrix and leads to deformation. This result in reduction of contact stress around fracture surfaces and increase in fracture aperture. Fluid rock interaction result in permeability evolutions in the fracture network and create new engineered fracture. Local aperture variation may play a strong role in reservoir thermal performance. When large faults are the main flow for fluid conduits, the modelling of fracture opening and closing are very crucial for predicting long term evolution of geothermal reservoir (Berkowitz et al., 2002). Cooling and overpressure resulted in reduction of the effective

normal stress and increase in fracture aperture. Fracture aperture increased near the injection well due to the contraction of solid and the induced effective stress were solid. Thermal contraction of the rock cause reduction of vertical compressive stress on the fracture wall and opening of the fracture. Fox et al (2015) investigated the effect of spatial aperture variation on the thermal performance of a discrete fractured geothermal reservoir and found that the degradation of thermal performance due to aperture variation was largest when the bore spacing was a larger fraction of the fracture diameter. Their results also showed that standard deviation of the apertures had the largest influence on thermal performance while the spatial correlation played a secondary role. Pandey et al (2016) believe that increase in rock matrix permeability will cause leakage of injected water and increase in matrix contraction due to cooling and thus aperture growth. Guo et al. (2016) also suggested that larger correlation lengths led to flow channelling when aperture alteration was induced by the thermal contraction of the rock matrix during heat extraction. Finally, Heda et al. (2018) found that lowering the young modulus will lead to a reduction in the stresses that are developed during the contraction of the matrix and lower fracture aperture.

# Chapter 2: Methodology

A fully coupled hydro-mechanical model is utilized to investigate the effect of aperture heterogeneity in a fractured reservoir. A 1-D permeability test is carried on a model from which the output flow is simulated. Then using Darcy's equation the equivalent permeability of the network is calculated. The model consists of the mechanical deformation due to the change in the external stress, flow through fracture and flow in the matrix which are calculated using darcy;s law. The mechanical model is elastic, the flow through fracture is laminar, and. The exchange of the fluid between fracture and rock matrix (leakoff) is ignored.

## 2.1 Computational Model

The model is developed by Salimzadeh et al. (2017) (2018), and it was built in Complex Systems Modelling Platform (CSMP) (Matthai et al., 2001). It yield the output flow from which the permeability is calculated using Darcy's equation. The linear algebraic equations are solved using SAMG which is an algebraic multigrid method for systems. The fractures are represented as 2-D surfaces in a 3-D domain. Quadratic triangles and tetrahydral are used to discretise the domain spatially using Galerkin finite element method. The fluid within the fracture applies hydraulic loading on the fracture surfaces so the fracture aperture, $a_f$ , is given by the differential displacement between the two faces of the fracture, $a_f = (\mathbf{u}^+ - \mathbf{u}^-).\mathbf{n}_c$, where $\mathbf{u}^+$ and $\mathbf{u}^-$ are the displacements of the two opposing faces of the fracture and nc is the outward unit normal to the fracture wall (on both sides of the fracture).

## 2.3 Discrete Fracture Network:

A ‘‘discrete fracture network” (DFN) refers to a computational model that represents the geometrical properties of each individual fracture explicitly such as orientation, size, position aperture and shape, and the topological relationships between each fractures and their sets. Unlike the conventional definition of DFNs that corresponds to stochastic fracture networks, the

term DFN here represents a much broader concept of any explicit fracture network model. Geological mapping is used to generate DFN and geomechanical simulation to represent different types of rock fractures including joints, faults, veins … In this study, the fracture are generated using an algorithm ( DFN generator) which calculate key parameters of a fracture population such as density, size distribution and connectivity. We study the effect of changing the following parameters on the equivalent permeability:

1. Subcritical Fracture Propagation index b
2. Size Distribution Of Initial Microfracture c
3. Output Intermediate Stage DFNs

# Chapter 3: Results

The computational domain used for the HM model is 3 km in x direction, 3 km in y direction and 0.1 km in z direction. The fractures are modelled as a rectangular surface. General values for rock and fluid properties used are listed in Table 1.

| Parameters | Model | Unit |
|---|---|---|
| Density ($\boldsymbol{\rho_f}$) | 1000 | $kg/m^3$ |
| Viscosity ($\boldsymbol{\mu}$) | 0.001 | Pa.s |
| Heat capacity ($\boldsymbol{C_f}$) | 850 | J/kg °C |
| Thermal conductivity ($\boldsymbol{\lambda_f}$) | 3.5 | W/m °C |
| Thermal expansion ($\boldsymbol{\beta_f}$) | 0.002 | 1/ °C |
| Compressibility ($\boldsymbol{c_f}$) | $5.11 \times 10^{-10}$ | $Pa^{-1}$ |
| Young's modulus ($E$) | 14.e9 | Pa |
| Poisson ratio ($\boldsymbol{v}$) | 0.37 | - |
| Porosity ($\boldsymbol{\phi}$) | i) 0.001 | - |
| Permeability ($\boldsymbol{k_m}$) | 1.e-15 | $m^2$ |
| Biot coefficient ($\boldsymbol{\alpha}$) | 1 | - |
| Initial contact aperture | - 1.e-3 | m |
| $\Delta P$ | 1 | Mpa |
| Average aperture | 1 | mm |

*Table 1: Rock and Fluid Properties*

The output flow refers to the fluid flow in the matrix and in the fracture:
$Q_t = Q_m + Q_t$ with

$Q_m = \frac{KmA\Delta P}{\mu L}$ and $Q_f = \frac{KfA\Delta P}{\mu L}$

Fracture permeability is function of the aperture and is calculated by $K_f = a^3/12$

## 3.1 Fracture Generation

This section shows the results of varying some parameters in the fracture generator in order to able to create different fracture geometries that will be imported into the model. The first parameter we modify is the subcritical index b which is classify into 3 categories:

a) **b < 5** : -Subcritical fracture propagation Population short fracture broad range of size distribution

b) **b > 15**: -Critical fracture propagation fracture population comprising a relatively small number of much longer fractures

c) **5 > b < 15** : Intermediate fracture propagation

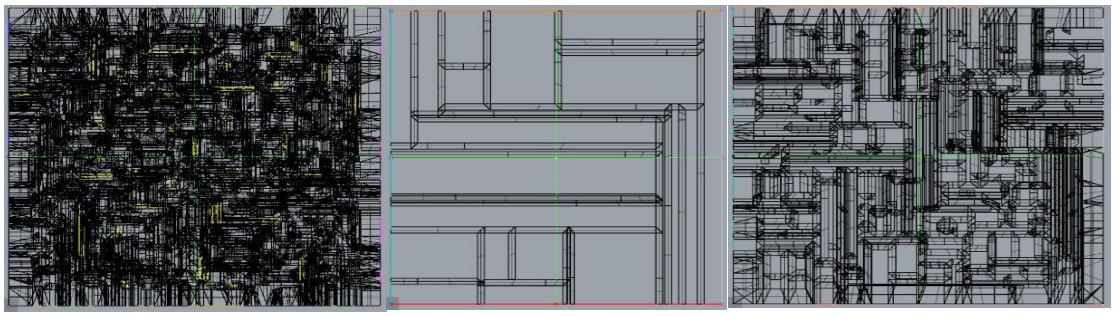

*Figure 1: Fractures representation according to the propagation index chosen (a, b and c)*

For fracture abundance measure, we use the $P_{32}$ parameter to characterize the fracture density which represents the area of the fractures over the volume of the rock mass.

$$P_{32} = \frac{area\ of\ fractures}{Volume\ of\ rock\ mass}$$

| b | $P_{32}$ ($m^{-1}$) | K (mD) |
|---|---|---|
| 5 | 0.051 | 1400 |
| 10 | 0.029 | 815 |
| 20 | 0.00028 | 12 |

*Table 2: Permeability and density values for each 3 different values of b*

By varying this parameter, we were able to create different sets of fracture from low density to high density network. Also, as the number of fracture increases, the permeability increases consistently.

The second parameter that was modified is the size Distribution of Initial Microfracture c: By increasing this parameter, the number of small fracture increases,. We compare the results with a fracture network of same density ($P_{32}$= 0.029) but with longer fractures (figure 2).


*Figure 2: Pressure propagation for 2 sets of fractures with same density and 2 different c values*

This shows that long fractures affects strongly the equivalent permeability even for same density network. It is more important to have a connected fracture network then to have high number of small fractures.

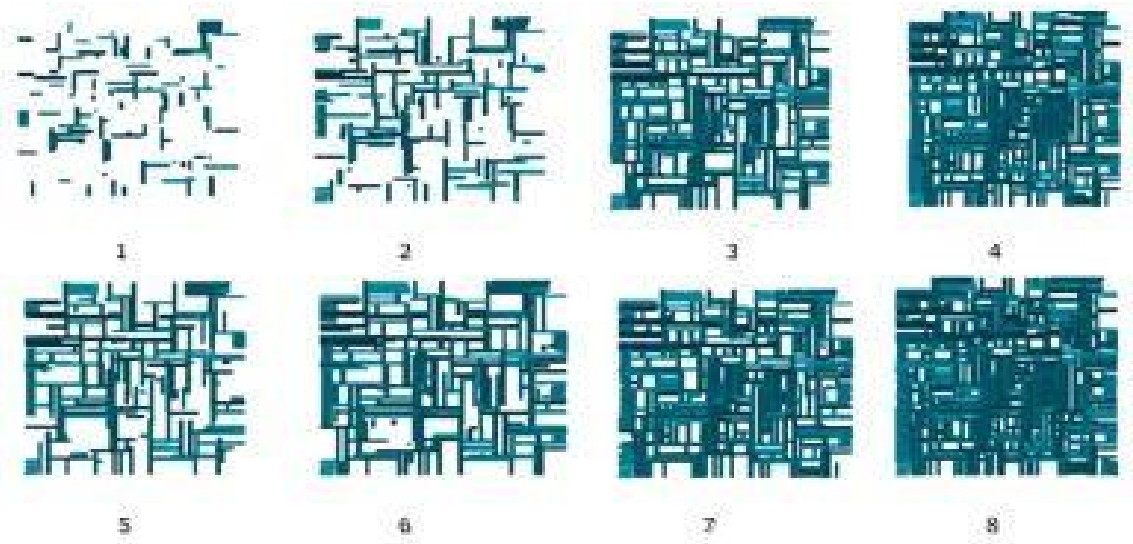


*Figure 3: 8 different stages of a fracture network generation*

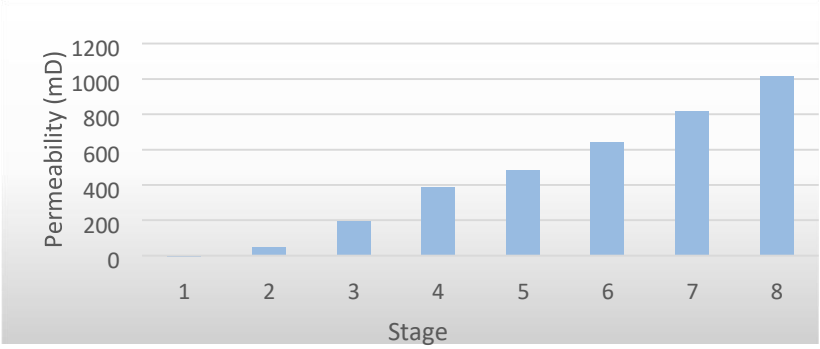


*Figure 4: Permeability value for each of the 8 stages*

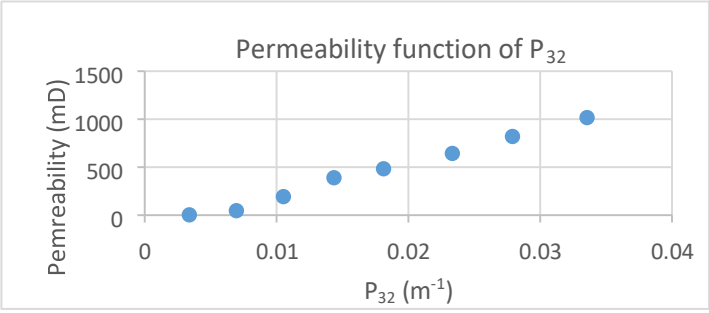


*Figure 5: Permeability variation in with respect to the density of each stage*

The fracture generator program was used in this study to create fractures with different orientation and intermediate stage to be able to characterize the effect of heterogeneity over low, intermediate and high density network

## 3.2 Aperture Heterogeneity:

In DFN modeling, rock fractures are described by smooth parallel plates. However, in nature, rock fractures have heterogeneous aperture distributions due to the rough surfaces. The apertures of a fracture had been found to typically follow under a given state of stress the gamma distribution or the log-normal distribution or a truncated Gaussian distribution. In our study we used the lognormal distribution (Figure 8).

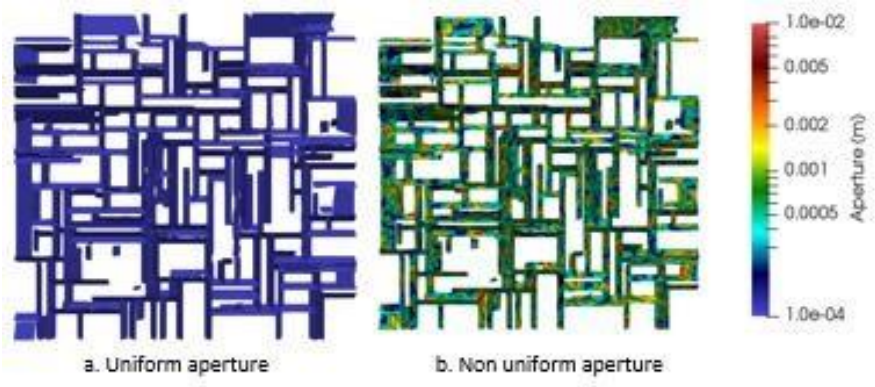


*Figure 6: fracture considering uniform aperture (a) and non-uniform (b)*

In order to investigate the effect of heterogeneity on the fracture network, we introduced the ratio

$$\frac{\text{K Homogeneous}}{\text{K Heterogeneous}}$$

Which represents the equivalent permeability of the system assuming uniform aperture (K homogeneous) over the permeability of the system assuming non uniform aperture (K heterogeneous)

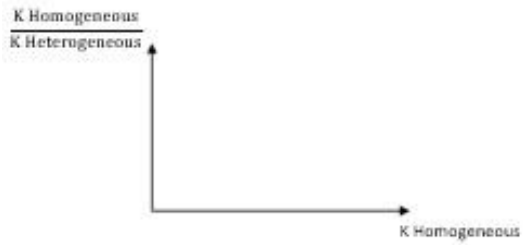


*Figure 7: variation of heterogeneity ratio with respect to the equivalent permeability assuming uniform aperture*

However, Every time a simulation is ran, it creates a new distribution which is slightly different from the previous for same standard deviation (figure 7). For this reason, many realization should be done for each simulation. In this work, we used 3 realization for each case.

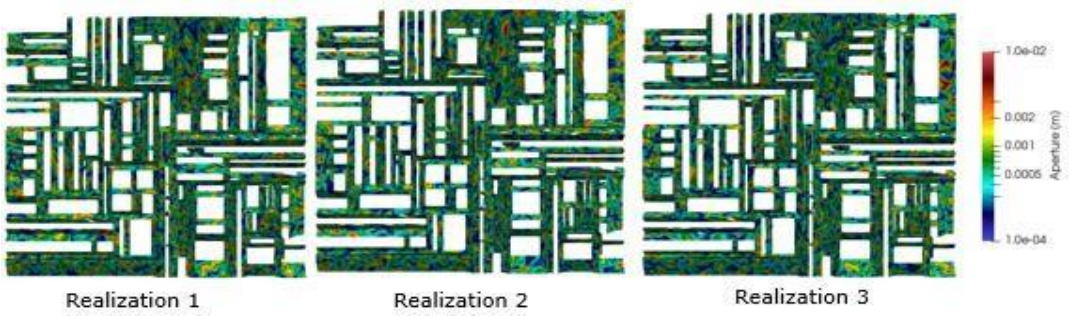


*Figure 8 3 different realizations for same fracture set and standard deviation*

| Realization | Permeability (mD) |
|---|---|
| 1 | 271 |
| 2 | 237 |
| 3 | 216 |

*Table 3: Permeability value for the 3 different realization*

Using the algorism discussed in section 2, four different sets of fracture were created with different geometries and distribution (figure 9).

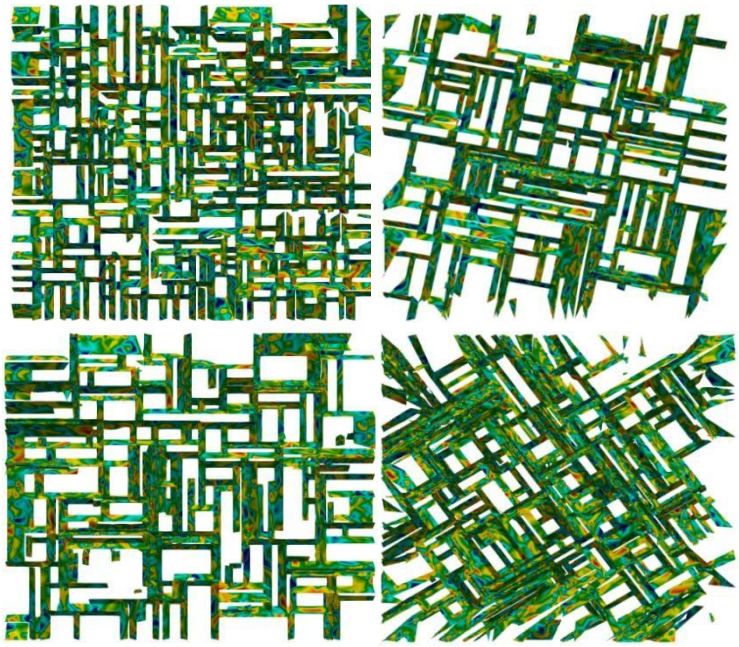

*Figure 9: 4 sets of fracture with different orientation and fracture lengths*

For each set, 8 different intermediate stages are created. The values for standard deviation we studied are 1, 2 and 5 mm. This will lead to 4 (sets)* 8 (stages) *3 (realization) * 3 (SD) = 288 and (8*4) for the uniform aperture which brings the total number of simulations to 320. This covers fractured networks ranging from low to high equivalent permeability. The mean aperture is 1mm, and we considered 3 different standard deviations 1, 2 and 5 mm. Apertures can varies from 0.1 mm till 10 mmm

| Parameters | Value |
|---|---|
| Mean | 1 mm |
| Standard Deviation | (1, 2 , 5) mm |
| Maximum Value | 10 mm |
| Minimum Value | 0.1 mm |

*Table 4 apertures parameters and values*

| Stages | K Homogeneous (mD) | K Heterogeneous (mD) 1 | K Heterogeneous (mD) 2 | K Heterogeneous (mD) 3 | Average (mD) | K homogeneous/ K Heterogeneous (SD=1) |
|---|---|---|---|---|---|---|
| 1 | 2.05658 | 2.04942 | 2.04514 | 2.04436 | 2.05658 | 1.00502 |
| 2 | 45.8455 | 26.97 | 44.7127 | 29.9422 | 45.8455 | 1.353374 |
| 3 | 193.787 | 119.563 | 107.632 | 147.515 | 193.787 | 1.551496 |
| 4 | 388.059 | 271.055 | 237.719 | 216.291 | 388.059 | 1.605617 |
| 5 | 480.916 | 325.924 | 324.025 | 417.779 | 480.916 | 1.351232 |
| 6 | 643.696 | 609.835 | 516.815 | 564.799 | 643.696 | 1.141677 |
| 7 | 818.824 | 722.325 | 671.873 | 705.986 | 818.824 | 1.169646 |
| 8 | 1014.06 | 987.797 | 967.81 | 1086.91 | 10.1406 | 0.999889 |

*Table 5: Results for set 1 for a standard deviation 1 mm and 3 realizations*

| Stages | K Homogeneous (mD) | K Heterogeneous (mD) 1 | K Heterogeneous (mD) 2 | K Heterogeneous (mD) 3 | Average (mD) | K homogeneous/ K Heterogeneous (SD=2) |
|---|---|---|---|---|---|---|
| 1 | 2.05658 | 2.03212 | 2.02566 | 2.0285 | 2.02876 | 1.013713 |
| 2 | 45.8455 | 18.2023 | 18.6225 | 15.8596 | 17.56147 | 2.610574 |
| 3 | 193.787 | 74.9728 | 78.5536 | 70.5307 | 74.6857 | 2.5947 |
| 4 | 388.059 | 202.014 | 131.048 | 143.413 | 158.825 | 2.443312 |
| 5 | 480.916 | 236.804 | 233.626 | 159.747 | 210.059 | 2.289433 |
| 6 | 643.696 | 450.45 | 367.165 | 331.571 | 383.062 | 1.680396 |

| | | | | | | |
|---|---|---|---|---|---|---|
| 7 | 818.824 | 630.459 | 586.585 | 760.363 | 659.1357 | 1.242269 |
| 8 | 1014.06 | 983.229 | 923.936 | 896.615 | 934.5933 | 1.085028 |

*Table 6: Results for set 1 for a standard deviation 2 mm and 3 realizations*

| Stages | K Homogeneous (mD) | K Heterogeneous (mD) 1 | K Heterogeneous (mD) 2 | K Heterogeneous (mD) 3 | Average (mD) | K homogeneous/ K Heterogeneous SD=5 (mm) |
|---|---|---|---|---|---|---|
| 1 | 2.05658 | 1.99488 | 2.01099 | 2.0047 | 2.003523 | 1.026482 |
| 2 | 45.8455 | 15.5531 | 14.1154 | 17.6026 | 15.75703 | 2.909526 |
| 3 | 193.787 | 51.9935 | 39.1191 | 58.843 | 49.9852 | 3.876888 |
| 4 | 388.059 | 100.408 | 134.217 | 265.502 | 166.709 | 2.327763 |
| 5 | 480.916 | 168.788 | 288.308 | 277.425 | 244.8403 | 1.964203 |
| 6 | 643.696 | 358.481 | 308.687 | 384.647 | 350.605 | 1.835958 |
| 7 | 818.824 | 609.027 | 485.14 | 492.155 | 528.774 | 1.548533 |
| 8 | 1014.06 | 819.354 | 808.432 | 804.997 | 810.9277 | 1.250494 |

*Table 7: Results for set 1 for a standard deviation 5 mm and 3 realizations*

We plot the results of set 1 in a graph and we obtain the following graph:

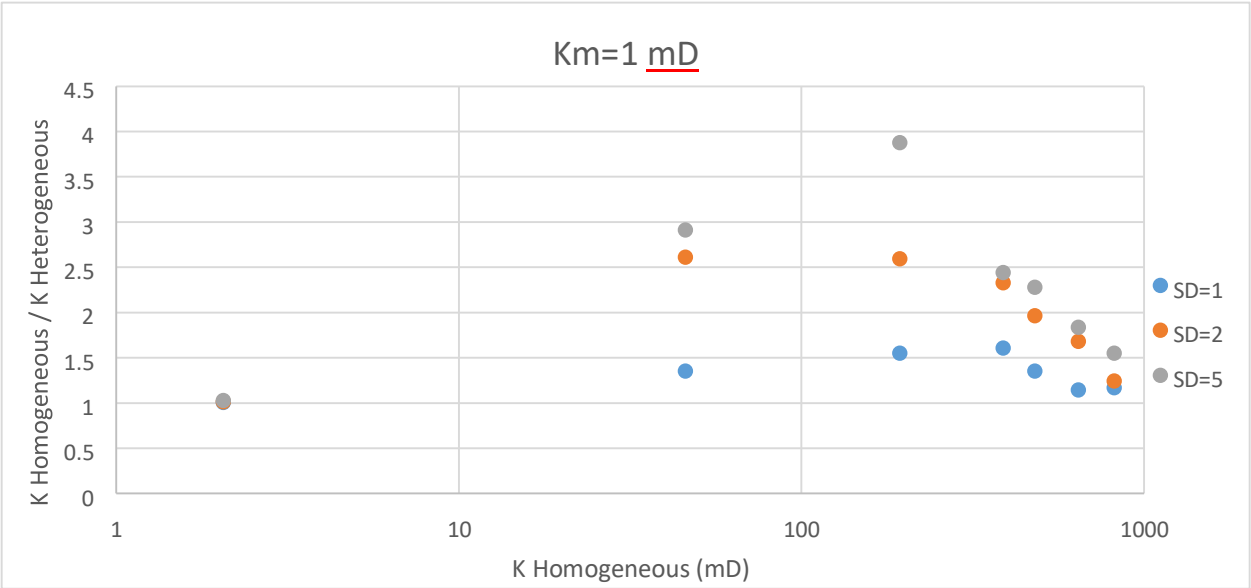


*Figure 10: Heterogeneity ratio with respect to the equivalent permeability for set 1*

We repeat the calculations for the 3 other sets:

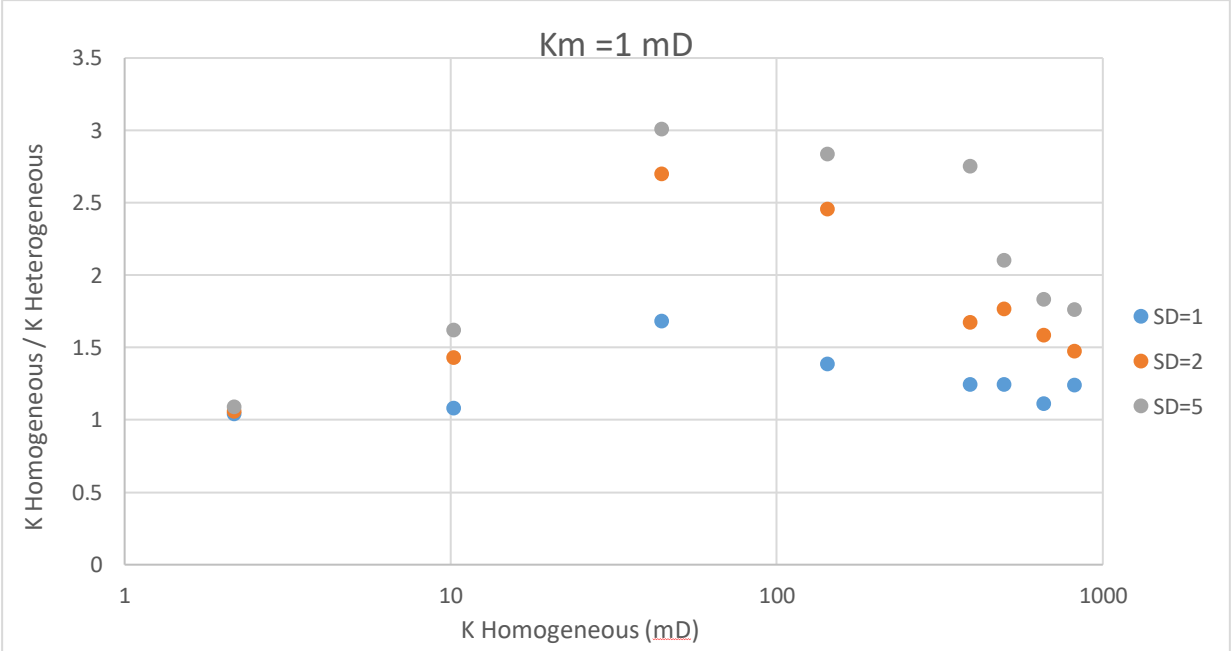


*Figure 11: Heterogeneity ratio with respect to the equivalent permeability for set 2*

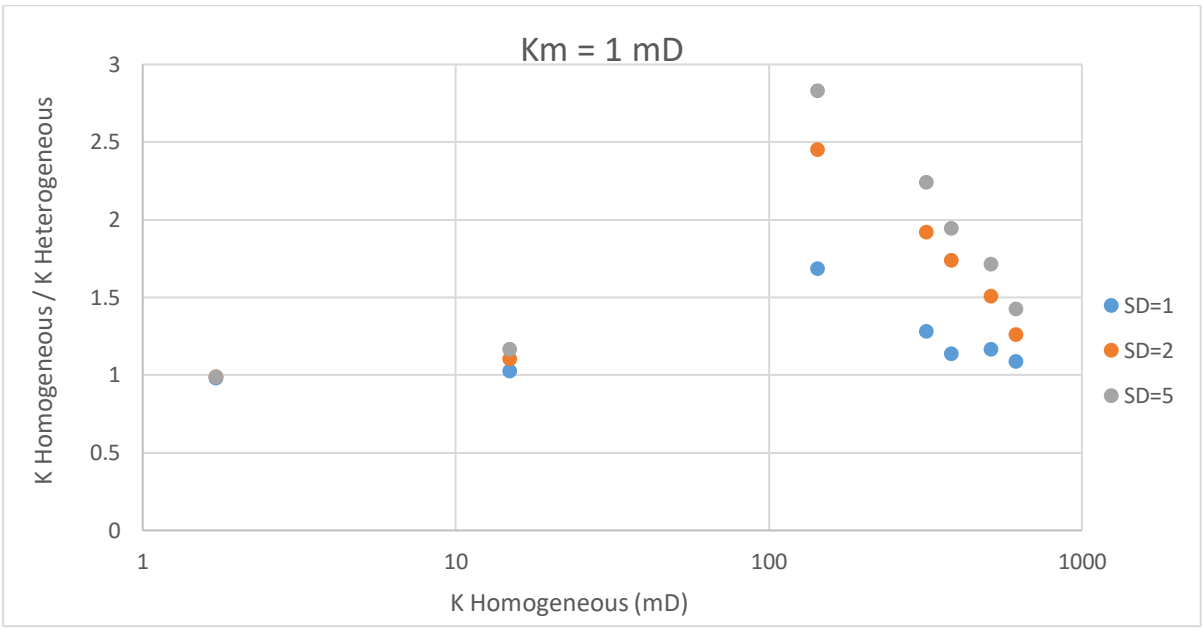


*Figure 12: Heterogeneity ratio with respect to the equivalent permeability for set 3*

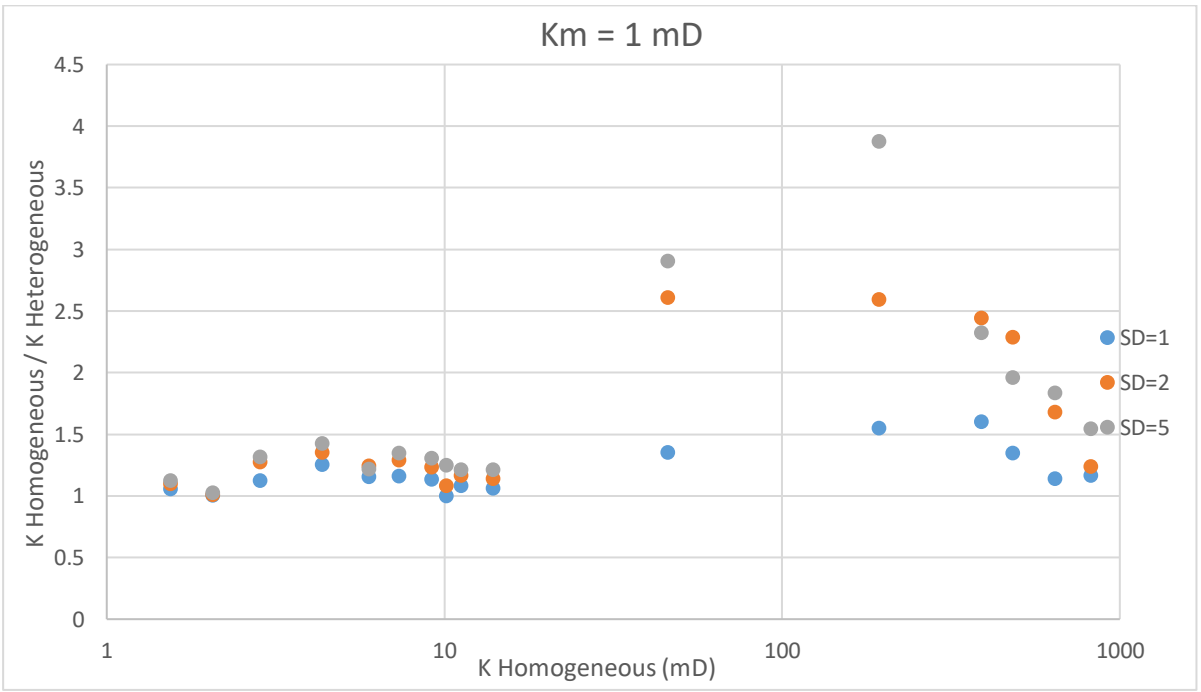


*Figure 13: Heterogeneity ratio with respect to the equivalent permeability for set 4*

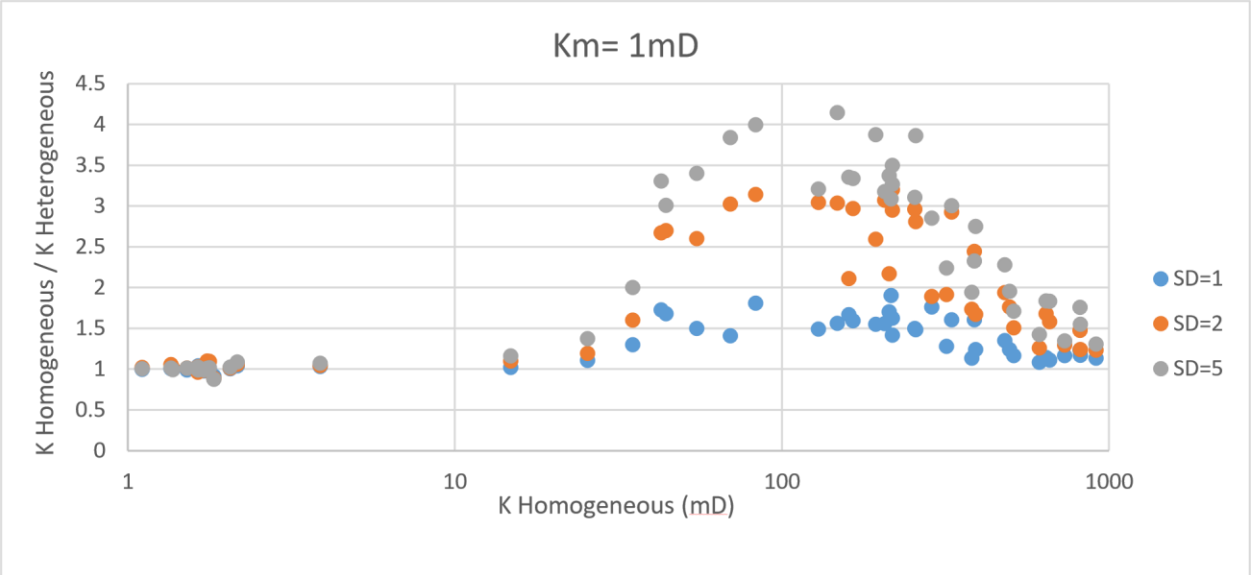


*Figure 14: Heterogeneity ratio with respect to the equivalent permeability for set 1*

### 3.2.1 Interpretation

At low fracture density, the effect heterogeneity is negligible for the 3 standard deviation as the permeability of the system depends only on the matrix's one. As the contribution of the fracture increased, the equivalent permeability of the system depends on the fracture's and the effect of heterogeneity start to increase up to a threshold where it starts to decrease again to become almost negligible at high fracture network. The effect of heterogeneity depends strongly on the standard deviation as it increase respectively where for SD=5 it has the highest effect. Higher standard deviation means higher variation the aperture which will lead to a lower equivalent permeability.

### 3.2.2 Discussion

Aperture heterogeneities below the network threshold tend to decrease the permeability medium and above this threshold, it tends to increase the permeability (ratio is decreasing, heterogeneous permeability increasing). The reason for this behavior is that it allows the fluid to select a path through the most transmissive fracture as more fractures intersect between themselves and offer additional larger transmissivity shortcuts and deviations, therefore enhancing the equivalent network permeability. Increasing the fracture density means increasing the number of alternative paths and progressively removing the limitations induced by smaller fracture apertures by allowing them to be bypassed. Below the threshold, the few number of fractures display a large number of bottle necks, which are expected to be highly sensitive to local apertures within fracture planes. A small reduction of the aperture around these bottle necks will strongly reduce the full network permeability, while an enhancement of the permeability (increase of the aperture) of the same zones will only slightly increase the network permeability.

However, it should be noted that 3 realization are not enough in order to fully characterize the behavior of heterogeneity at specific permeability, In order to predict the exact effect of heterogeneity at a specific permeability, many sets should be created until the sum of the ratio over the number of sets becomes constant.

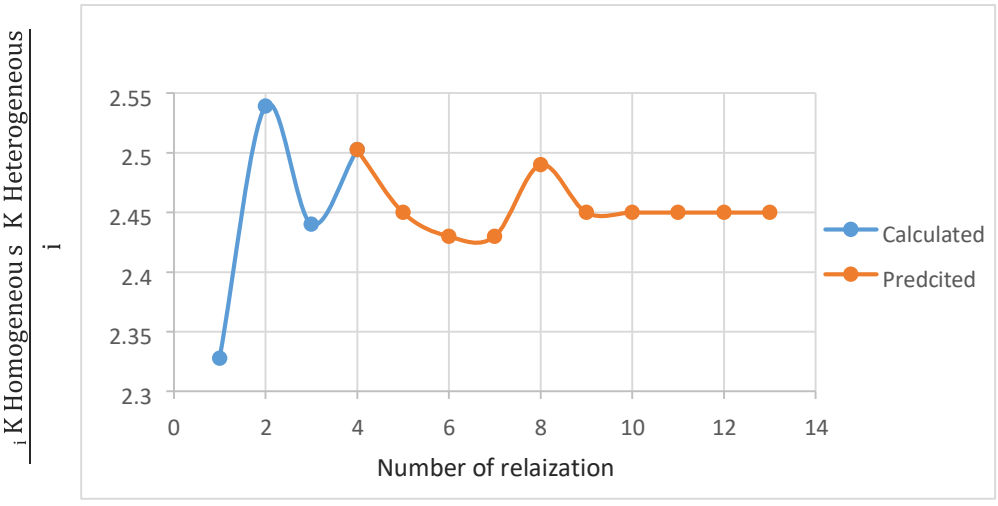


*Figure 15: Calculated and predicted heterogeneity ratio for set 1 for 380 mD*

## 3.3 Effect Of Matrix Permeability

In this section, we repeat the simulations of case 1 but with a matrix permeability to 100 mD. Results are shown in the table below:

| Stage | Km=1 mD | Km=100 mD | Change (%) |
|---|---|---|---|
| 1 | 2.056 | 154.57 | 98 |
| 2 | 45.84 | 284.68 | 84 |
| 3 | 193.79 | 433.77 | 55 |
| 4 | 388.06 | 597.98 | 36 |
| 5 | 480.92 | 733 | 34 |
| 6 | 643.696 | 915.151 | 35 |
| 7 | 818.824 | 1120.21 | 26 |
| 8 | 1014.06 | 1390.03 | 27 |

*Table 8: Comparison of the equivalent permeability by increasing Km to 100 mD*

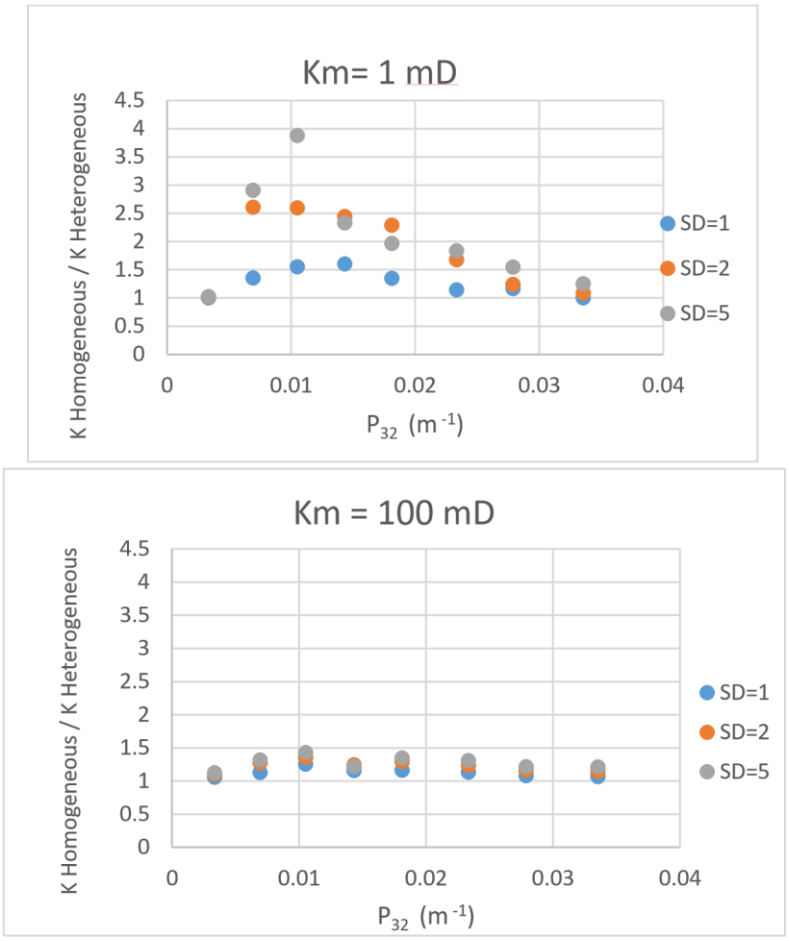


*Figure 16: Comparison between for heterogeneity results using km=1 mD and km= 100 mD*

The effect of heterogeneity decrease when matrix permeability increase and is independent on standard deviation and is almost negligible for the different fracture densities. The effect of increasing matrix permeability is critical at low fracture densities as the contribution of the fracture to the equivalent permeability is small.

## 3.4 Effect Of Mechanics:

Fluid rock interaction result in permeability evolutions in the fracture network and create new fracture. Changes in external stress could alter the fracture dimension, by changing the global or

local aperture height. For example, compression between the two rock surfaces tends to reduce the aperture height and could even close some apertures when two surfaces are in contact. As a result, changes in fracture dimension are not just altering the width of flow paths, but could also provide extra or eliminate pre-existing flow paths. Kang et al. [2016] showed the emergence of preferential flow paths and anomalous transport behavior across a stressed applied fracture. In this section we apply a 1.5 Mpa stress our model, so the aperture of the aperture will be function of the normal contact stress according to barton bandis.

$$a_f^c = a_f^o - \frac{a\sigma_n}{1+b\sigma_n}$$

where, $a_f{}^o$ = 0.0012m is the fracture aperture at zero or a minimal effective stress, $a_f{}^c$ is the aperture at the current effective stress $\sigma_n{}'$ while $a = 1.6 \times 10^{-10}$ and $b = 1.333 \times 10^{-7}$ are model parameters. As the effective stress is computed from the contact traction in the mechanical model, it couples the mechanical deformation of the fracture with the fluid flow through the fracture.

We repeat the simulations for set 1 by accounting for mechanical deformation and the results are shown in figure 18.

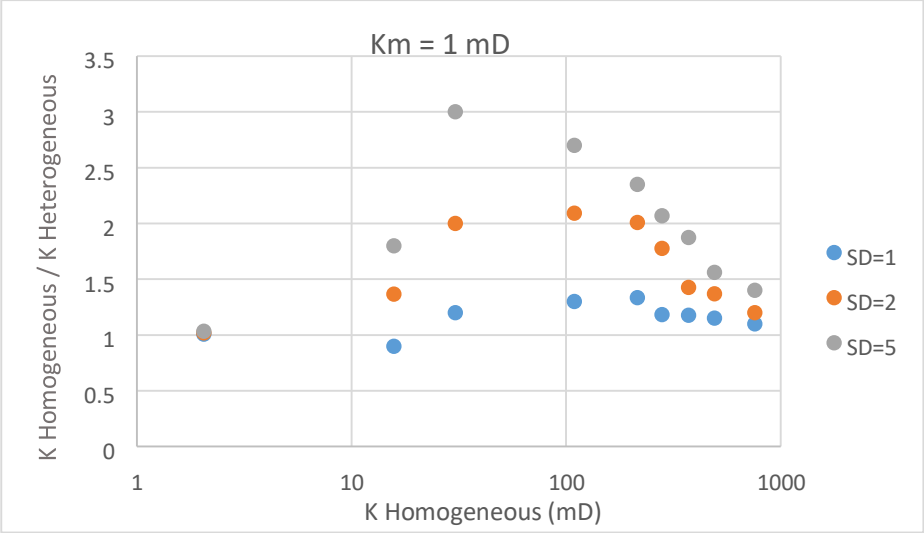


*Figure 17 Heterogeneity ratio with respect to the equivalent permeability (with mechanics)*

Then, we plot the same graph the results for set 1 for the standard deviation of 5 mm for the 2 cases: with mechanics and without mechanics (figure 18)

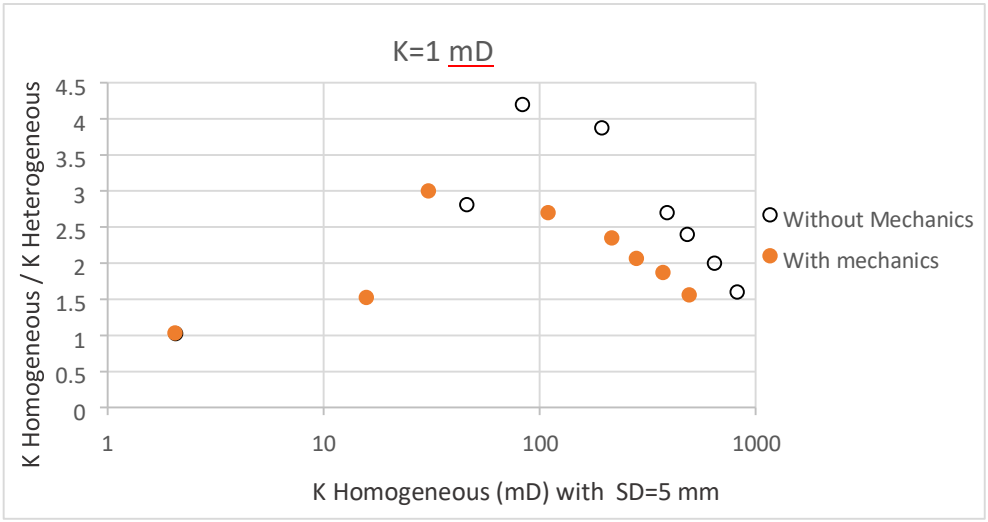


*Figure 18: Heterogeneity ratio with respect of equivalent permeability for set 1 for SD=5 mm*

The contact stress apply to the model results in to contraction of the matrix and lowering of the fracture aperture. The behavior of the curve is the same as the one without mechanics, however it will leads to a decrease in the equivalent permeability as the apertures of the fractures are reduced. At high fracture densities, the addition of mechanics did not affect the ratio of heterogeneity ratio because as previously stated, this ratio decrease at high fracture densities. As the compression magnitude increases, the effective permeability decreases. This result was expected because as the increased compression narrowed the apertures, providing smaller cross-section area for fluid to flow. In particular, it was observed that fractures that have high effective permeability at reference compression state are less affected by compression.

### 3.4.1 Matrix Pressure:

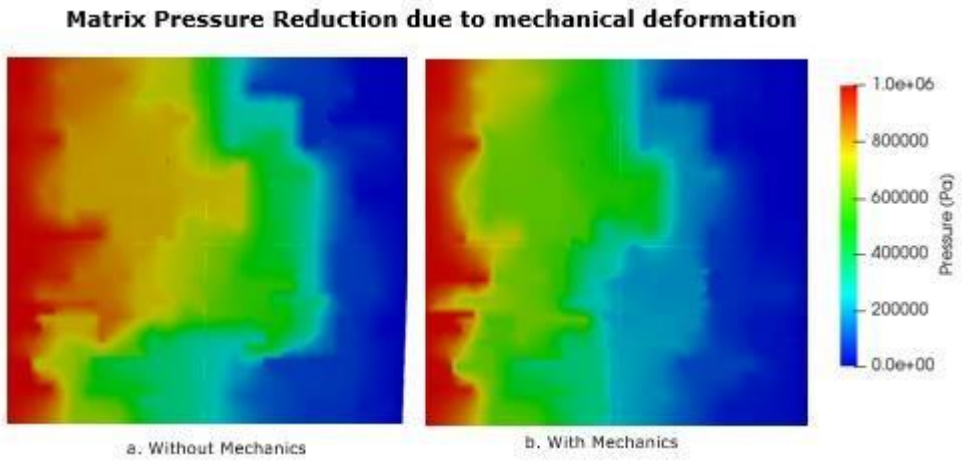


*Figure 19: Pressure propagation in the model for a (without mechanics) and b (with mechanics)*

The decrease in the pressure propagation in case b is due to aperture reduction which will most likely generates obstacles or aperture closures thus the flow will propagate over higher interval in a as fractures are more connected.

# Chapter 4: Conclusion

In this study, a coupled hydro-mechanical model was developed to investigate the effect of aperture heterogeneity on the equivalent permeability in a fractured network. The model account for mechanical deformation, fluid flow in the fracture and fluid flow in the matrix. Fractures ranging from low to high density medium were generated and imported to the model were a 1-D permeability test were carried out. The model is firstly tested with a uniform aperture in the fractures, i.e. assuming the fractures considered as parallel plates. In the second step the apertures were distributed according to the log normal distribution and the heterogeneity was measured as the ratio between the permeability between the two cases. The effect of increasing matrix permeability was also analyzed and finally the mechanical deformation was taken into consideration by applying a 1.5 Mpa contact stress on the model. Results showed that neglecting aperture heterogeneity tends to overestimate the equivalent permeability. Also, Fracture density strongly affects the change in heterogeneity ratio, as this ratio increase with network density up to a threshold where it starts to decrease until it becomes negligible. The standard deviation in the aperture plays also a fundamental role in the heterogeneity as the higher the standard deviation, the higher the effect of heterogeneity. The simulations for each case were repeated three times in order to further validate the results.

The effect of heterogeneity decreases when matrix permeability increases as less fractures contribute to the total flow. Finally including mechanics resulted aperture closure in some parts due to the stress applied on the model which will lead to flow path reduction and thus making the fracture network less connected. Therefore, the equivalent permeability will be lower.

The next step should be in determining the threshold at which the ratio of heterogeneity start to decrease, thus the requirement for more simulations for each case, and finally taking into account the heat transfer flow in the fracture and in the matrix to check the effect of the thermal stress on the heterogeneity in a fractured network.

‘

# References


Berkowitz, B. (2002). Characterizing flow and transport in fractured geological media: A review. *Advances in water resources*, *25*(8-12), 861-884.

Bisdom, K., Bertotti, G., & Nick, H. M. (2016). The impact of in-situ stress and outcrop-based fracture geometry on hydraulic aperture and upscaled permeability in fractured reservoirs. *Tectonophysics*, *690*, 63-75.

Bogdanov, I. I., Mourzenko, V. V., Thovert, J. F., & Adler, P. M. (2007). Effective permeability of fractured porous media with power-law distribution of fracture sizes. *Physical Review E*, *76*(3), 036309.

Cladouhos, T., Petty, S., Foulger, G., Julian, B., & Fehler, M. (2010). Injection induced seismicity and geothermal energy. *GRC Transactions*, *34*, 1213-1220.

Canbolat, S., & Parlaktuna, M. (2018). Analytical and visual assessment of fluid flow in fractured medium. *Journal of Petroleum Science and Engineering*, *173*, 77-94.

Dreuzy, J. R., Méheust, Y., & Pichot, G. (2012). Influence of fracture scale heterogeneity on the flow properties of three-dimensional discrete fracture networks (DFN). *Journal of Geophysical Research: Solid Earth*, *117*(B11).

Ebigbo, A., Lang, P. S., Paluszny, A., & Zimmerman, R. W. (2016). Inclusion-based effective medium models for the permeability of a 3D fractured rock mass. *Transport in Porous Media*, *113*(1), 137-158.

Fox, D. B., Koch, D. L., & Tester, J. W. (2015). The effect of spatial aperture variations on the thermal performance of discretely fractured geothermal reservoirs. *Geothermal Energy*, *3*(1), 21

Gong, J., & Rossen, W. R. (2017). Modeling flow in naturally fractured reservoirs: effect of fracture aperture distribution on dominant sub-network for flow. *Petroleum Science*, *14*(1), 138-154

Gudmundsdottir, H., & Horne, R. N. Reservoir Characterization and Prediction Modeling Using Statistical Techniques. *Dimension (xyz)*, *1000*, m3.

Guo, B., Fu, P., Hao, Y., Peters, C. A., & Carrigan, C. R. (2016). Thermal drawdown-induced flow channeling in a single fracture in EGS. *Geothermics*, *61*, 46-62.

Jafari, A., & Babadagli, T. (2013). Relationship between percolation–fractal properties and permeability of 2-D fracture networks. *International Journal of Rock Mechanics and Mining Sciences*, *60*, 353-362.

Jarrahi, M., & Holländer, H. (2017). Numerical simulation of flow heterogeneities within a real rough fracture and its transmissivity. *Energy Procedia*, *125*, 353-362.

Ji, S. H., Park, Y. J., & Lee, K. K. (2011). Influence of fracture connectivity and characterization level on the uncertainty of the equivalent permeability in statistically conceptualized fracture networks. *Transport in porous media*, *87*(2), 385-395.

Jonoud, S., Wennberg, O. P., Larsen, A., & Casini, G. (2013). Capturing the effect of fracture heterogeneity on multiphase flow during fluid injection. *SPE Reservoir Evaluation & Engineering*, *16*(02), 194-208.

Li, Y., Shang, Y., & Yang, P. (2018). Modeling fracture connectivity in naturally fractured reservoirs: A case study in the Yanchang Formation, Ordos Basin, China. *Fuel*, *211*, 789-796.

Ma, J. H. Y., Li, Y. E., & Cheng, A. (2017). The effects of aperture distribution and compression on transport properties in rock fractures. In *SEG Technical Program Expanded Abstracts 2017* (pp. 3945-3949). Society of Exploration Geophysicists.

Masihi, M., King, P. R., & Nurafza, P. R. (2008). Connectivity prediction in fractured reservoirs with variable fracture size: analysis and validation. *SPE Journal*, *13*(01), 88-98.

Matthäi, S. K., & Belayneh, M. (2004). Fluid flow partitioning between fractures and a permeable rock matrix. *Geophysical Research Letters*, *31*(7).

Namdari, S., Baghbanan, A., & Habibi, M. J. (2016, January). Effects of matrix permeability and fracture density on flow pattern in dual porous rock masses. In *ISRM International Symposium-EUROCK 2016*. International Society for Rock Mechanics and Rock Engineering.

Salimzadeh, S., Paluszny, A., & Zimmerman, R. W. (2017). Three-dimensional poroelastic effects during hydraulic fracturing in permeable rocks. *International Journal of Solids and Structures*, *108*, 153-163.

Salimzadeh, S., Paluszny, A., Nick, H. M., & Zimmerman, R. W. (2018). A three-dimensional coupled thermo-hydro-mechanical model for deformable fractured geothermal systems. *Geothermics*, *71*, 212224.

Sarkar, S., Toksoz, M. N., & Burns, D. R. (2004). *Fluid flow modeling in fractures*. Massachusetts Institute of Technology. Earth Resources Laboratory.

Sun, J., & Schechter, D. S. (2014, October). Optimization-based unstructured meshing algorithms for simulation of hydraulically and naturally fractured reservoirs with variable distribution of fracture

aperture, spacing, length and strike. In *SPE Annual Technical Conference and Exhibition*. Society of Petroleum Engineers.

Vik, H. S., Salimzadeh, S., & Nick, H. M. (2018). Heat recovery from multiple-fracture enhanced geothermal systems: The effect of thermoelastic fracture interactions. *Renewable Energy*, *121*, 606-622.

Welch, M., & Luthje, M. (2018, June). Controls on Fracture Density and Size: Insights from Dynamic Modelling. In *80th EAGE Conference and Exhibition 2018*.

Yang, Z., Niemi, A., Fagerlund, F., & Illangasekare, T. (2013). Two-phase flow in rough-walled fractures: Comparison of continuum and invasion-percolation models. *Water resources research*, *49*(2), 993-1002.